



Published in final edited form as:

*Proc SPIE Int Soc Opt Eng.* 2018 February ; 10578: . doi:10.1117/12.2295631.

## SVA: Shape variation analyzer

Priscille de Dumast<sup>a</sup>, Clement Mirabel<sup>a</sup>, Beatriz Paniagua<sup>b</sup>, Marilia Yatabe<sup>a</sup>, Antonio Ruellas<sup>a</sup>, Nina Tubau<sup>a</sup>, Martin Styner<sup>c</sup>, Lucia Cevidanes<sup>a</sup>, and Juan C. Prieto<sup>c</sup>

<sup>a</sup>University of Michigan, Ann Arbor, United States

<sup>b</sup>Kitware, Carrboro, United States

<sup>c</sup>University of North Carolina, Chapel Hill, United States

### Abstract

Temporo-mandibular osteo arthritis (TMJ OA) is characterized by progressive cartilage degradation and subchondral bone remodeling. The causes of this pathology remain unclear. Current research efforts are concentrated in finding new biomarkers that will help us understand disease progression and ultimately improve the treatment of the disease. In this work, we present Shape Variation Analyzer (SVA), the goal is to develop a noninvasive technique to provide information about shape changes in TMJ OA. SVA uses neural networks to classify morphological variations of 3D models of the mandibular condyle. The shape features used for training include normal vectors, curvature and distances to average models of the condyles. The selected features are purely geometric and are shown to favor the classification task into 6 groups generated by consensus between two clinician experts. With this new approach, we were able to accurately classify 3D models of condyles. In this paper, we present the methods used and the results obtained with this new tool.

### Keywords

Temporo-mandibular osteo arthritis; deep learning; classification; artificial intelligence

## 1. INTRODUCTION

Osteoarthritis (OA), the most prevalent arthritis worldwide, is associated with significant pain and disability and affects 15% of adults at any given time.<sup>1</sup>

The complex pathogenesis of temporomandibular joint (TMJ) OA remains unclear to this day, and understanding its progression challenges experts given the different morphological patterns of bone resorption and formation observed in its various stages. The disease may evolve into repair and morphological adaptation, but also into aggressive bone destruction and functional impairment. Patients with OA present a variety of symptoms including pain, limited jaw movement, grinding, clicking, and deviation on opening. Figure 1 shows the mandibular condyles. There is no method to quantify morphology for early diagnosis, assessment of disease progression and treatment effects. The symptoms are different from

patient to patient, i.e., TMJ OA may be in a quiet state until is set of by an array of events, or it may be painful from the start. However, recent work quantifying condylar morphology revealed differences between OA and asymptomatic condyles.<sup>2</sup>

The goal of this work is to develop a noninvasive technique to provide information about bony changes and disease changing in TMJ OA, using shape analysis. Given the complexity of such heterogeneous conditions and current clinical, biological, and imaging data in arthritis of the temporomandibular joint, there is a compelling need for more efficient software tools to facilitate these analyses. To answer this challenge, we developed Shape Variation Analyzer (SVA) using a neural network to classify morphological variations using 3D models of the mandibular condyle. In this work, we created 7 different categories for the classification task: 0. Normal, 1. Overgrowth, 2. Close to Normal, 3. Degeneration 1, 4. Degeneration 2, 5. Degeneration 3, 6. Degeneration 4; Figure 2 shows samples of each group with the average shape of the control group.

The development of this tool did not consist only on building and training a neural network but also the pre-processing steps to prepare the data, which include generating 3D models of the condyles,<sup>3</sup> improve shape correspondence,<sup>4</sup> and extract shape features from the 3D models. The process of extracting shape features are detailed in this paper. The features are selected because they are purely geometric and they do not depend on the position nor the orientation of the model, which may vary across the different groups in the population, and may introduce bias for the analysis.

## 2. MATERIALS

The study group consists of 268 TMJ joints (163 TMJ OA, 105 asymptomatic controls), obtained from Cone Beam Computed Tomography (CBCT) scans (i-CAT Next Generation, 120kV, 18.66mA). TMJ OA joints were subdivided, by consensus between 2 clinicians, into 6 subgroups based in morphological variability, compared to the average control morphology. Figure 3 shows the distribution of samples across the different groups in TMJ OA.

## 3. METHODS

### 3.1 Model creation

The CBCT images are segmented using a semi-automated method in ITK-SNAP.<sup>5</sup> The software allows manual editing to clean the segmentation. Figure 4 shows a screen-shot of the application with different orthogonal slices of the image. Using EasyClip\* (a module included in 3DSlicer), the condylar models are simultaneously cropped to define the condylar region of interest. The cropped segmentation maps are used to generated regular tessellations.

Spherical harmonics representation point distributed models (SPHARM-PDM)<sup>6</sup> is used to generate a mesh with 1002 points, via spherical mapping and spherical parametrization of

---

\*<https://www.slicer.org/wiki/Documentation/4.8/Extensions/EasyClip>

the input segmentation maps. SPHARM- PDM generates a regular mesh, as show in Figure 5(a). After the models have the same number of points and a regular mesh, we proceed to place landmarks in the 3D models. The landmarks are placed in homologous regions for all individuals. Figure 6 shows a condyle with the landmarks placed on the surface. These landmarks are used to generate a tessellation with correspondent points employing a group-wise registration method.<sup>4</sup> Figure 7 shows the condylar models aligned where regions in the 3D model correspond across the population.

### 3.2 Feature extraction

Using the aligned 3D models, an average model is created for each group. The features that led to higher accuracy in classification include the normal vectors, mean curvature of the surface, and the distances to the average meshes. In general, the input data for our network has shape  $N * n_{pt} * n_{feat}$  where  $N$  is the batch size during training,  $n_{pt} = 1002$  and  $n_{feat} = 10$ . These features do not include any information about position and are purely geometric.

Figure 8 shows the different features computed for every model in the population. Video 9 shows some features displayed on the surface of the condyle.

As shown in Figure 3, the groups have a significant difference in the number of samples, i.e., an imbalanced dataset. Training a neural network with an imbalanced dataset is known as the class imbalance problem.<sup>7</sup> If a neural network is trained with an imbalanced dataset, it will learn to identify the majority class more often. In order to have a balance dataset, we use a synthetic minority over-sampling technique (SMOTE).<sup>8</sup>

Figure 10 shows the first two principal components plotted before and after SMOTE resampling. After SMOTE, each class has 105 data points and is now suitable to train a neural network. The next section will show the results of training and classification of our neural network.

## 4. RESULTS

The neural network has 4 hidden layers with [4096, 2048, 1024, 512] neurons, a drop out layer with probability 0.5 and softmax layer with 7 outputs. The learning rate was set to  $1^{-5}$ . The network was trained for 100 epochs and the batch size was set to 32. The SVA training is shown in Figure 11. The maximum accuracy during training was 93%. The dataset was subdivided in two sets, training and testing in a 80/20 ratio. The testing data was not used at any point during training and it will be used to test if the trained network generalizes well for unseen data samples. Using the testing dataset, the accuracy achieved was 95%.

## 5. CONCLUSION

SVA is new tool to analyze shape variation using deep neural networks. The results presented here indicate that using shape features only favors the classification task, i.e., we do not include any information about position or orientation of the model. This classification approach seems promising, as it may help us increase our understanding about shape

changes that TMJ OA patients undergo during the course of the disease. The source code repository is available at <https://github.com/DCBIA-OrthoLab/ShapeVariationAnalyzer>

Future work will focus on including additional predictors/features of the disease in the neural network training (e.g., clinical data, behavioral or biochemical). Clinical and behavioral data has been acquired through questionnaires, while biochemical data has been acquired through a protein analysis in saliva and plasma samples. Including these may contribute to improve the classification power of the neural network.

## Supplementary Material

Refer to Web version on PubMed Central for supplementary material.

## References

1. Kalladka M, Quek S, Heir G, Eliav E, Mupparapu M, Viswanath A. Temporomandibular joint osteoarthritis: diagnosis and long-term conservative management: a topic review. *The Journal of Indian Prosthodontic Society*. 2014; 14(1):6–15. [PubMed: 24604992]
2. Cevidanes L, Hajati AK, Paniagua B, Lim P, Walker D, Palconet G, Nackley A, Styner M, Ludlow J, Zhu H, et al. Quantification of condylar resorption in temporomandibular joint osteoarthritis. *Oral Surgery, Oral Medicine, Oral Pathology, Oral Radiology, and Endodontology*. 2010; 110(1):110–117.
3. Paniagua B, Cevidanes L, Walker D, Zhu H, Guo R, Styner M. Clinical application of spharmpdm to quantify temporomandibular joint osteoarthritis. *Computerized Medical Imaging and Graphics*. 2011; 35(5):345–352. [PubMed: 21185694]
4. Lyu I, Kim SH, Seong JK, Yoo SW, Evans AC, Shi Y, Sanchez M, Niethammer M, Styner MA. Group-wise cortical correspondence via sulcal curve-constrained entropy minimization. *Information processing in medical imaging: proceedings of the... conference*. 2013; 23:364. NIH Public Access. [PubMed: 24683983]
5. Yushkevich PA, Piven J, Cody Hazlett H, Gimpel Smith R, Ho S, Gee JC, Gerig G. User-guided 3D active contour segmentation of anatomical structures: Significantly improved efficiency and reliability. *Neuroimage*. 2006; 31(3):1116–1128. [PubMed: 16545965]
6. Styner M, Oguz I, Xu S, Brechbühler C, Pantazis D, Levitt JJ, Shenton ME, Gerig G. Framework for the statistical shape analysis of brain structures using spharmpdm. *The insight journal*. 2006; (1071):242. [PubMed: 21941375]
7. Japkowicz N, Stephen S. The class imbalance problem: A systematic study. *Intelligent data analysis*. 2002; 6(5):429–449.
8. Chawla NV, Bowyer KW, Hall LO, Kegelmeyer WP. Smote: synthetic minority over-sampling technique. *Journal of artificial intelligence research*. 2002; 16:321–357.

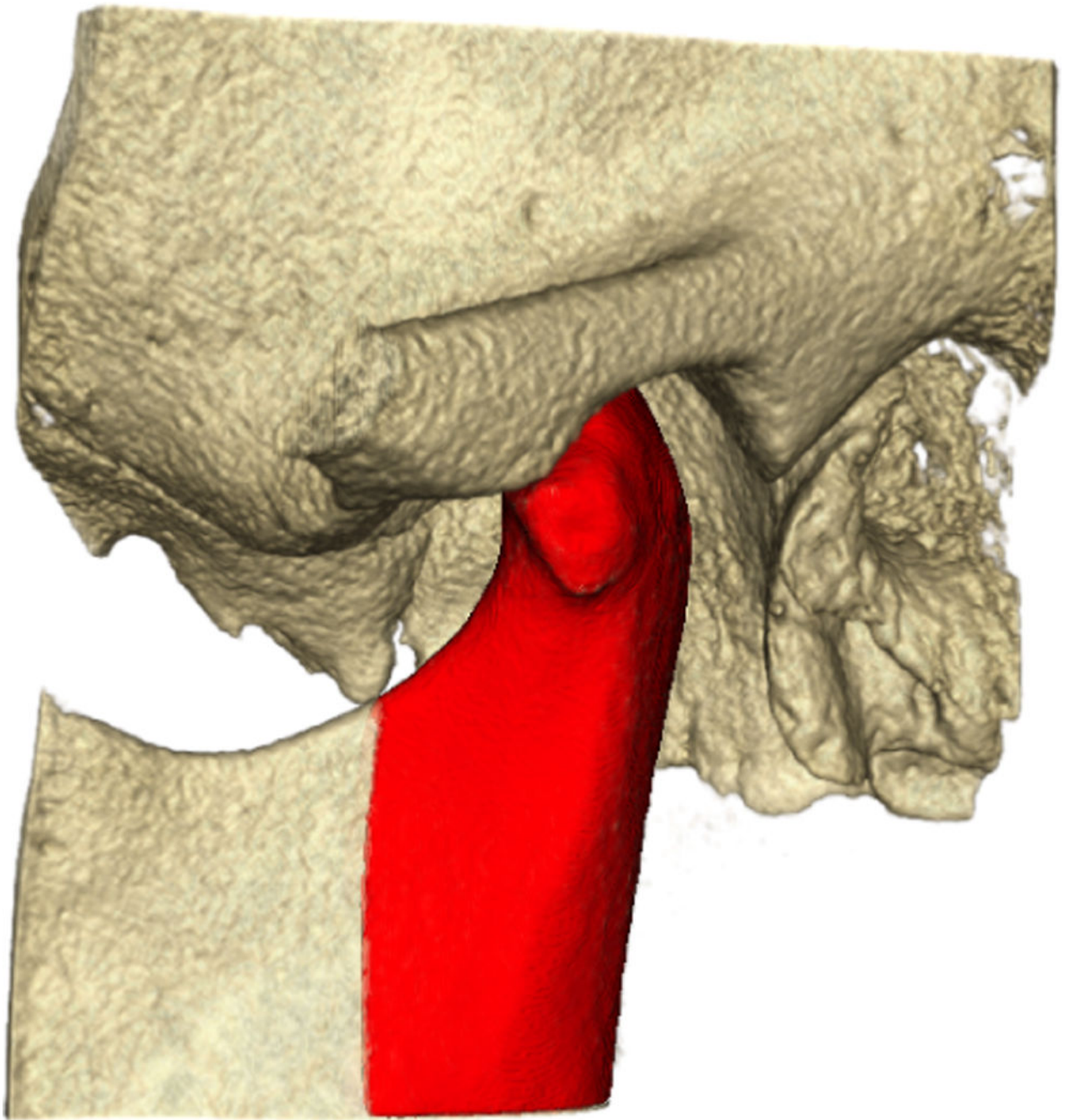


**Figure 1.**  
Volume rendering of CT image. Mandibular condyles in red.

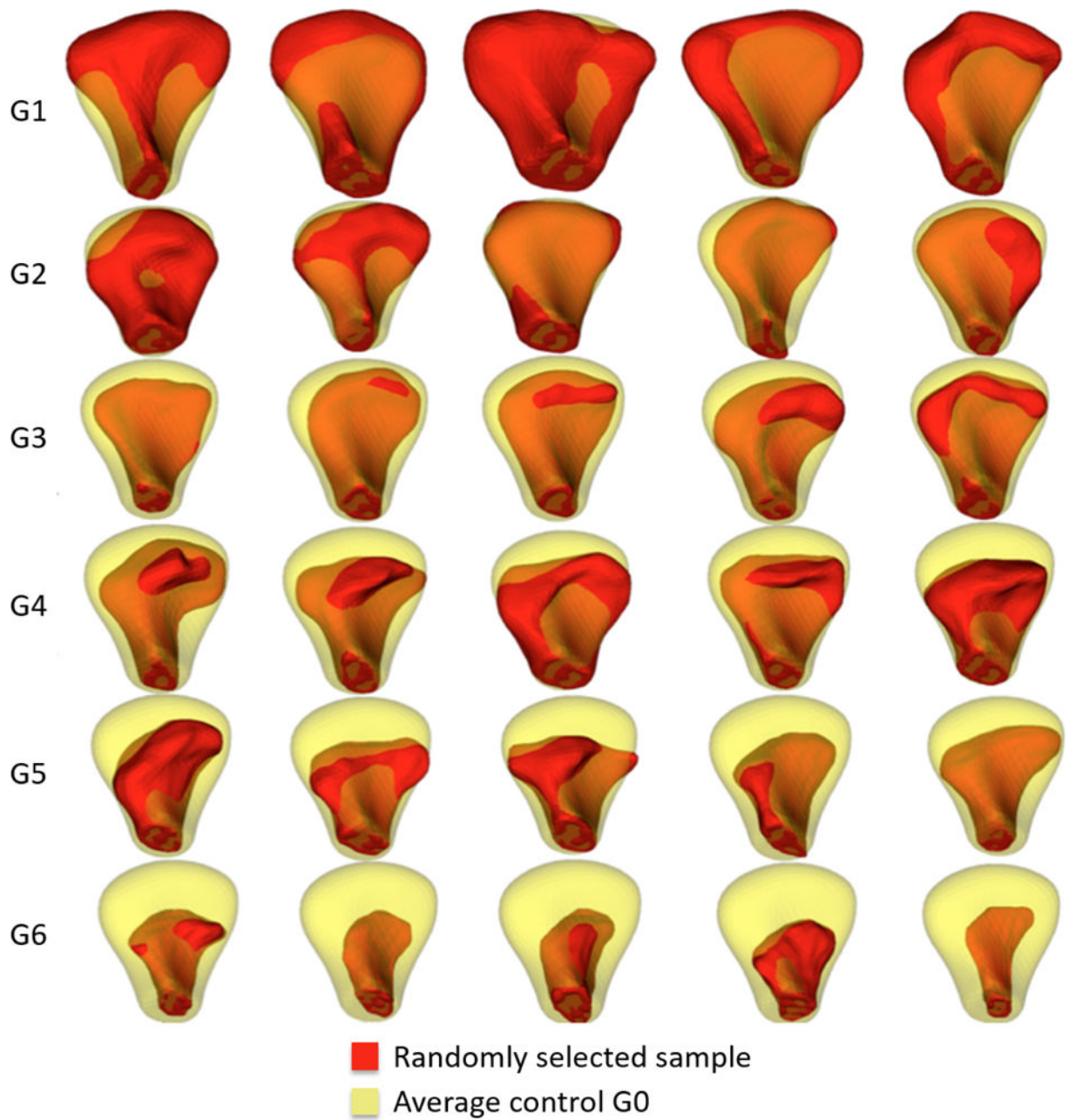


**Figure 2.**

Randomly selected subject samples for each group shown in red. In yellow, the average shape from the control group rendered transparent. G1. Overgrowth, G2. Close to Normal, G3. Degeneration 1, G4. Degeneration 2, G5. Degeneration 3, G6. Degeneration 4

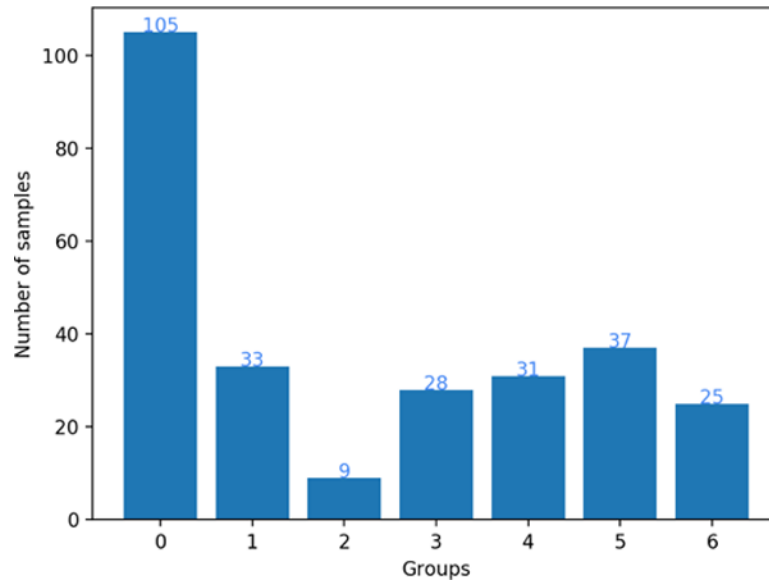


**Figure 3.** Distribution of condyles in the different groups. G0. Control, G1. Overgrowth, G2. Close to Normal, G3. Degeneration 1, G4. Degeneration 2, G5. Degeneration 3, G6. Degeneration 4

Author Manuscript

Author Manuscript

Author Manuscript

Author Manuscript

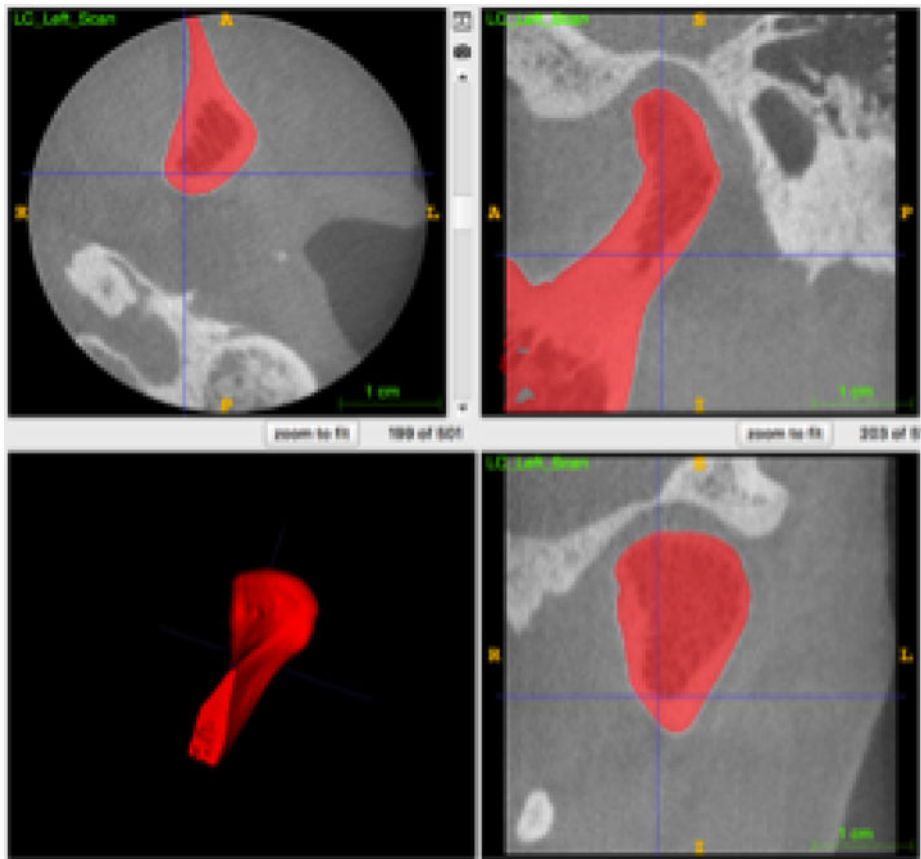


**Figure 4.**  
Manual segmentation of Condyles using ITK-SNAP



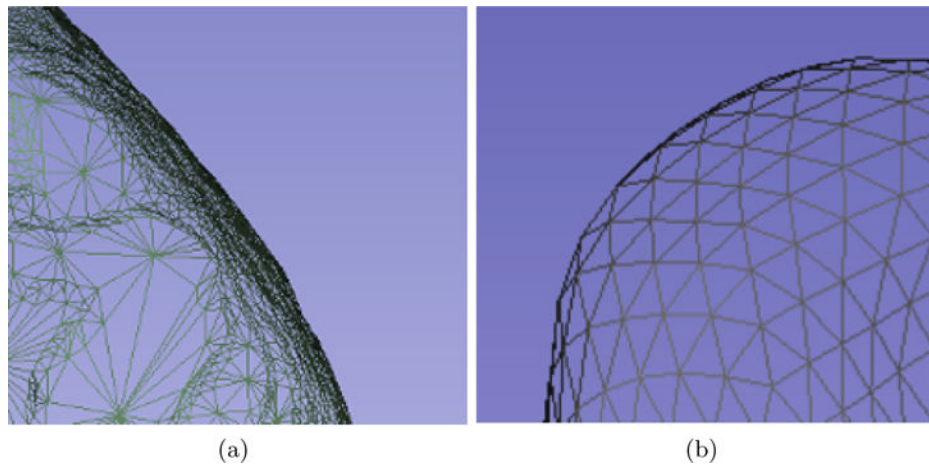


**Figure 5.** Figure (a) shows a condylar model generated with marching cubes. Figure (b) shows a condylar model after the parameterization via spherical harmonics. The tessellation is regular, i.e., equal area, and the models contain the same number of points across the population.

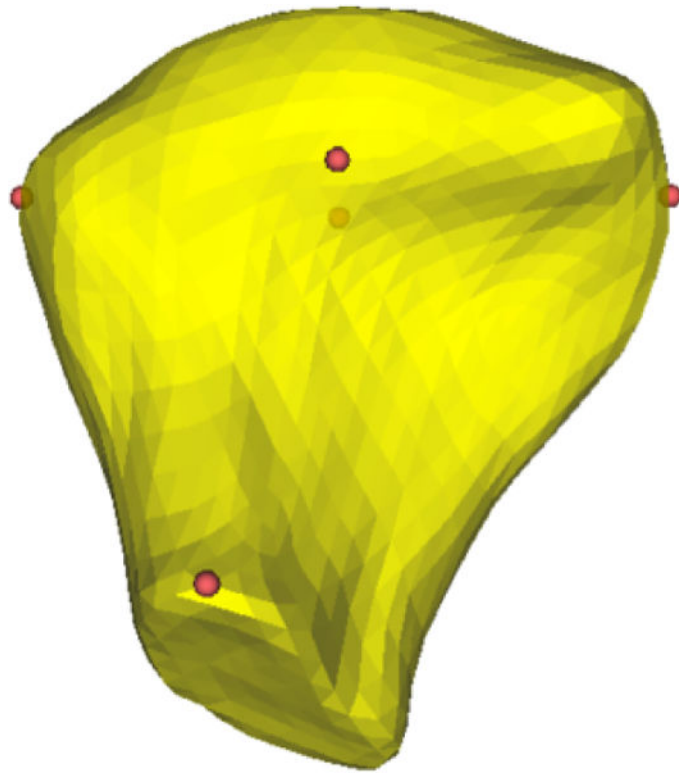


**Figure 6.**  
Landmarks in red, displayed in the surface of a condyle 3D model.

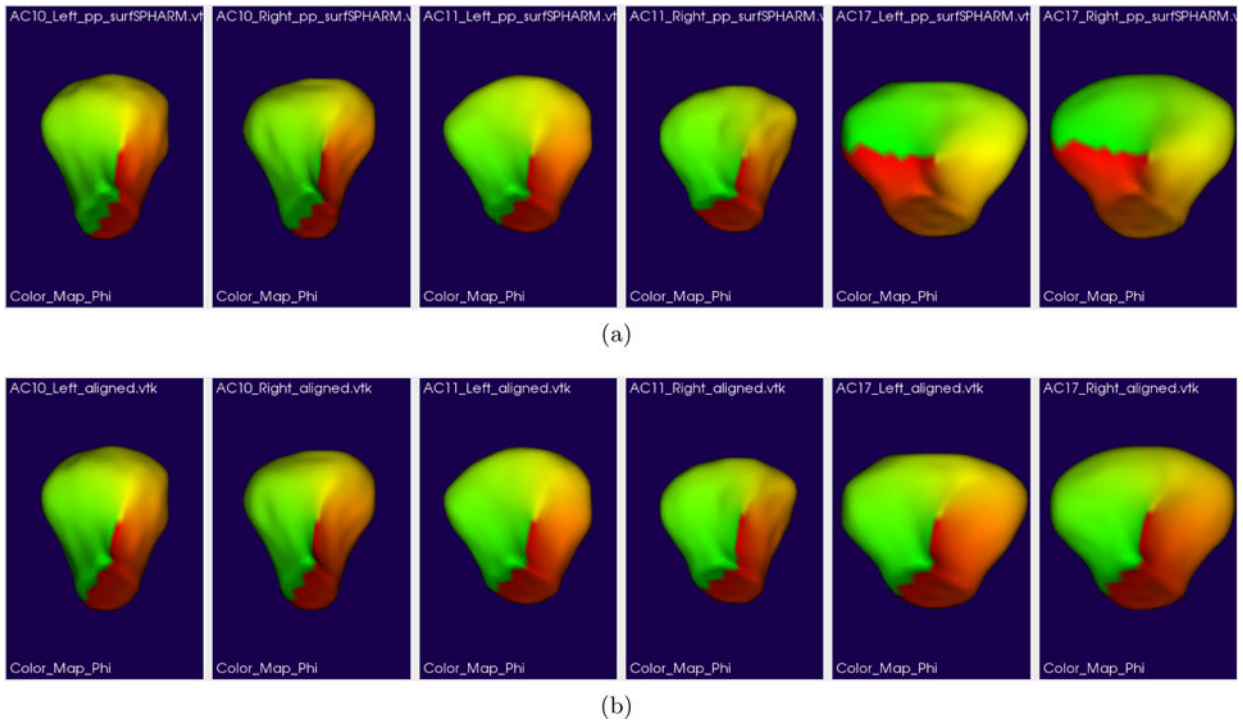


**Figure 7.** Group-wise correspondence (GROUPS). Figure (a) shows the models generated by SPHARM-PDM. The spherical parameterization produced by SPHARM and the landmarks are used to generate 3D models that have correspondent points across subjects. The rainbow color map in the 3D models encode the location. Figure (b) shows the 3D models after GROUPS processing, similar colors are found at every point in the model across all the samples in the population.

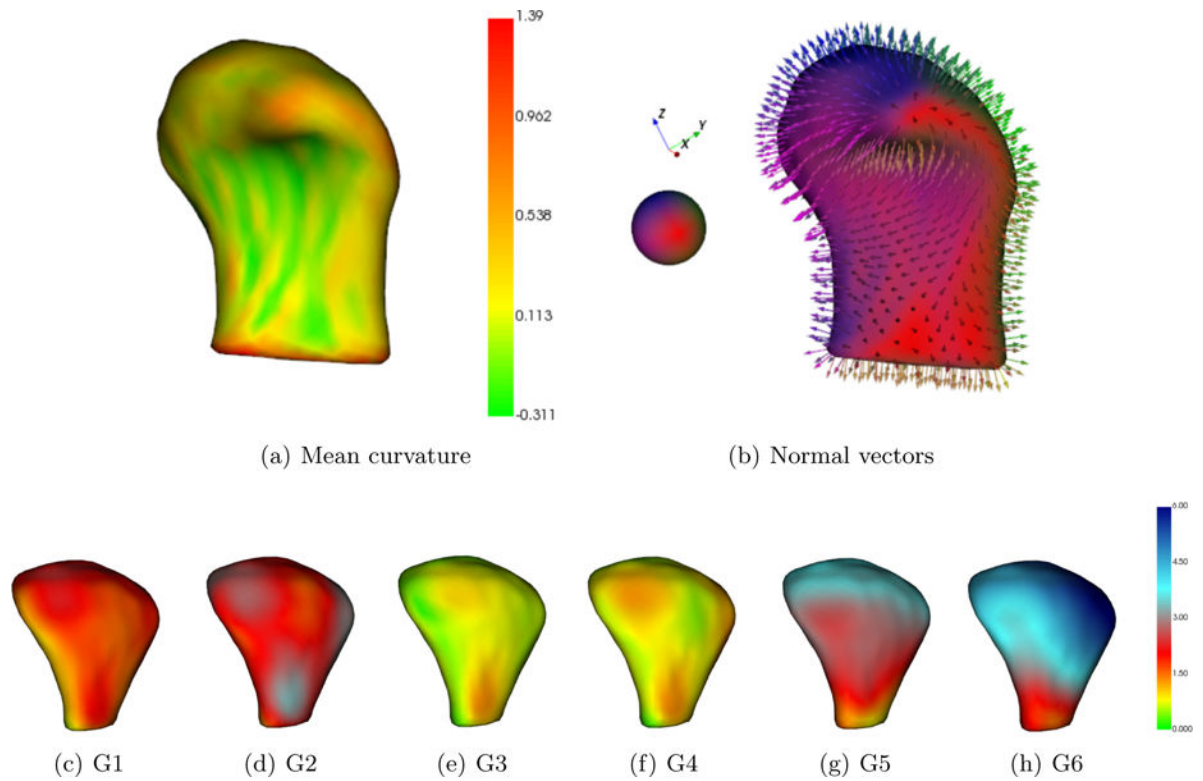
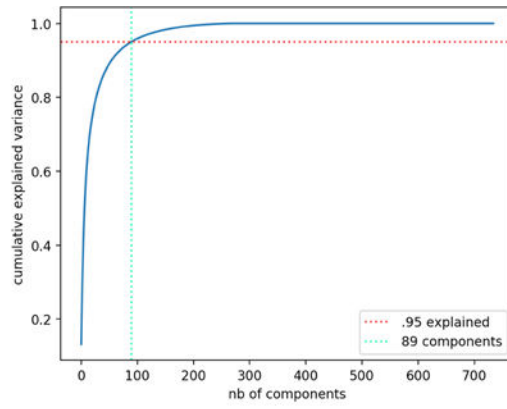


**Figure 8.**

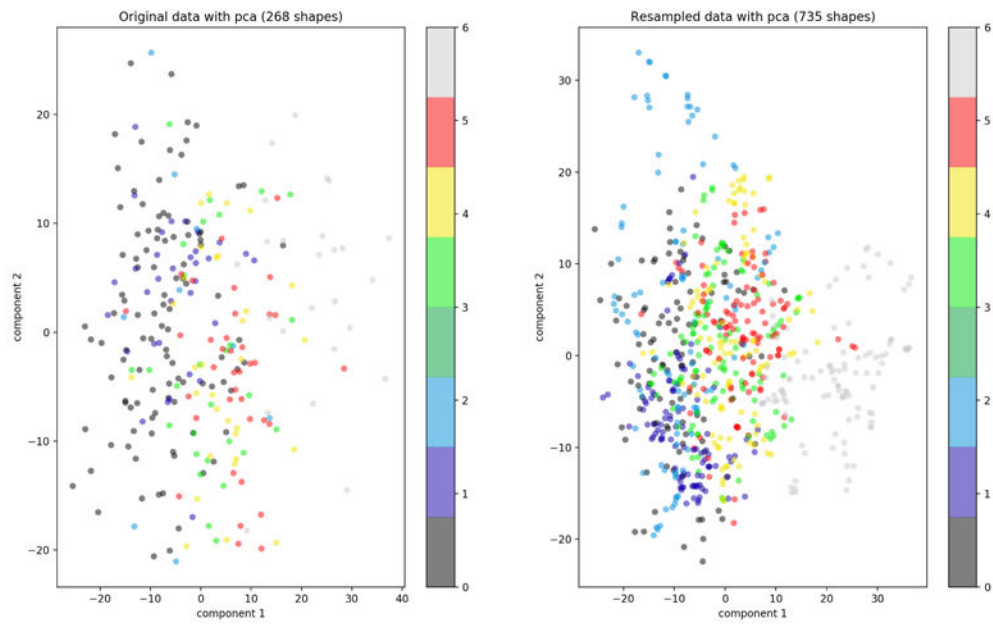
Visualization of the features computed for every condyle model at every point. Figure (a) shows the mean curvature of a model. Figure (b) shows normal vectors, color coded for direction. Figures (c)-(h) show color coded distance of every point to the average model of that particular group. In total the number of features is 10 for every point in the model.



**Figure 9.** <http://dx.doi.org/doi.number.goes.here>. This video shows a set of computed features on the surface of the condyle.



(a) Principal component analysis (PCA) of the original dataset (268). 89 components are necessary to explain 95% of the variance.



(b) SMOTE on feature space. The first two principal components are used to plot the datasets.

**Figure 10.**  
After resampling with SMOTE, each group has 105 data points.

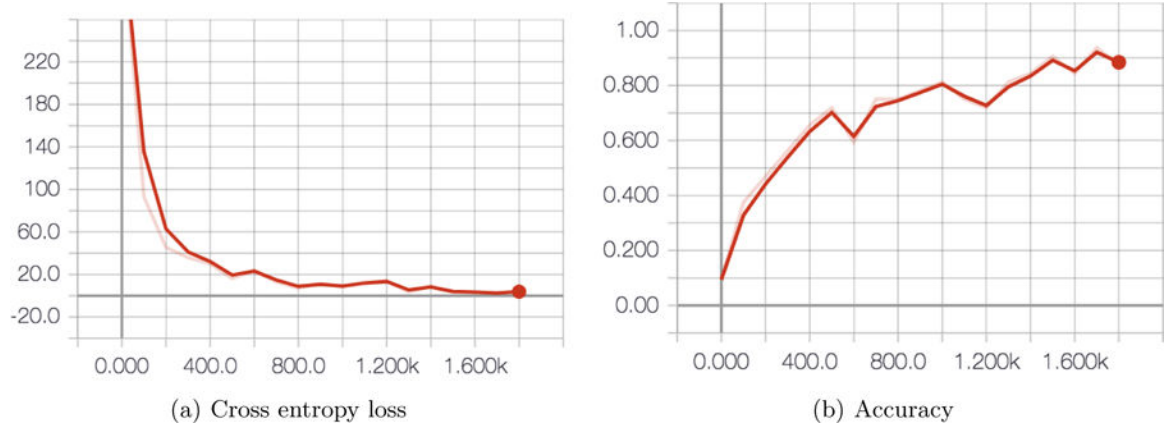


**Figure 11.** Cross entropy loss function and accuracy during training.

Author Manuscript

Author Manuscript

Author Manuscript

Author Manuscript